

# Experimental validation of two voltage regulation strategies for boost converters in wind systems

Belkasem Imodane, Mohamed Benydir, Brahim Bouachrine, Mohamed Ajaamoum,  
Kaoutar Dahmane

Laboratory of Engineering Sciences and Energy Management (LASIME), Ibn Zohr University, National School of Applied Sciences,  
Agadir, Morocco

## Article Info

### Article history:

Received Jun 23, 2024

Revised Oct 2, 2024

Accepted Oct 23, 2024

### Keywords:

Boost converter

DSP board

Experimental validation

Fuzzy logic control

Sliding mode control

Wind power systems

## ABSTRACT

This study provides an experimental validation of two advanced control methods, sliding mode control (SMC) and fuzzy logic control (FLC) for regulating the DC bus voltage in a permanent magnet synchronous generator (PMSG) wind turbine system using a boost converter. Initially, MATLAB/Simulink simulations are used to assess the system's behavior in an ideal environment, where various operating conditions and disturbances are modeled to test the robustness of the control algorithms. Subsequently, real experiments are conducted using a physical prototype of a boost converter and a LAUNCHXL-F28069M DSP board to evaluate the system's behavior under real-world scenarios. The evaluation focuses on system stability, tracking accuracy, and response time under various wind turbine operating conditions. The experimental results reveal that SMC outperforms FLC in terms of rapidity, precision, and hardware implementation. Additionally, SMC offers significant advantages in achieving superior performance metrics, such as improved dynamic response and enhanced overall system stability, making it a more effective choice for practical wind energy applications. This experimental validation simplifies the selection of optimal control strategies for wind energy systems.

*This is an open access article under the [CC BY-SA](https://creativecommons.org/licenses/by-sa/4.0/) license.*



## Corresponding Author:

Belkasem Imodane

Laboratory of Engineering Sciences and Energy Management (LASIME), Ibn Zohr University

National School of Applied Sciences

80000 Agadir, Morocco

Email: b.imodane@uiz.ac.ma

## 1. INTRODUCTION

To effectively integrate sustainable energy into power grids, advanced power conversion techniques optimize energy transfer and ensure grid reliability [1], [2]. Boost power converters address challenges such as voltage mismatches between renewable sources and grid requirements by increasing source voltages, improving the efficiency of renewable resources, reducing transmission losses, and enhancing grid reliability [3]-[6]. The stability of DC-DC boost converters is crucial, particularly in the case of variable input voltages from wind turbines and solar systems, to ensure reliable performance under a variety of conditions [7]-[10].

Multiple studies explore control techniques for DC-DC power converters. Proportional integral derivative (PID) controllers provide high precision but are sensitive to input fluctuations [11], [12]. Proportional resonant control (PRC) offers fast response, disturbance resistance, and low computational load, but has limitations like sensitivity to uncertainties and inapplicability to non-minimum phase systems [13], [14]. Model predictive control (MPC) ensures rapid response but is sensitive to parameter variations [15]. Neural network-based controllers enhance dynamic performance but require extensive training and are

computationally intensive [16]. Fuzzy logic control (FLC) uses fuzzy logic to manage uncertainties in renewable sources, ensuring stability [17], [18]. Sliding mode control (SMC) offers robustness against uncertainties and disturbances, maintaining stability with rapid voltage tracking [19], [20].

Virtual simulations have made it possible to validate control methods, but differences often appear in real-world applications. Simulations, which assume ideal conditions, neglect factors such as component variability, switching losses and temperature effects. It is therefore essential to validate control strategies under realistic conditions, taking into account environmental variability, disturbances and hardware limitations. This study aims to validate sliding mode control (SMC) and fuzzy logic control (FLC) under realistic conditions using a prototype 20 W DC/DC power converter. Tests include variable input voltages (7 V to 11.5 V) and implementation on the LAUNCHXL-F28069M DSP board.

This paper is structured as, section 2 covers the modeling and sizing of the DC/DC power converter in continuous conduction mode. Section 3 presents the controller design. Section 4 discusses simulation results, experimental findings, and comparative analysis. The final section presents concluding remarks and suggestions for future research.

## 2. SIZING AND MATHEMATICALE MODELING OF BOOST CONVERTER

A typical example of a non-isolated boost power converter is presented in Figure 1. This architecture is widely used in renewable energy applications like wind power [21], where the reference output voltage needs to be tracked and adjusted. The circuit of a DC/DC boost converter presented in Figure 2 includes a DC voltage source designated by  $V_{in}$ , a controlled switch represented by  $T$ , an inductance represented by  $L$ , a diode  $D$ , a filter capacitor expressed as  $C$ , and a load. We will analyze the operation of the converter in continuous conduction mode (CCM) by examining the different states based on the conduction of the switch  $T$ .

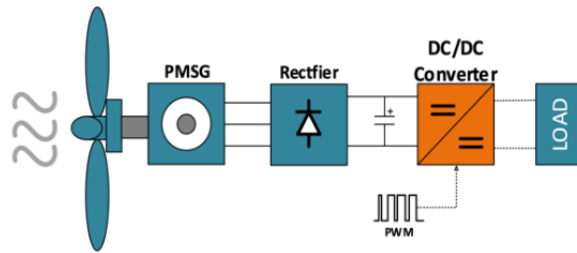


Figure 1. Overview of the system studied

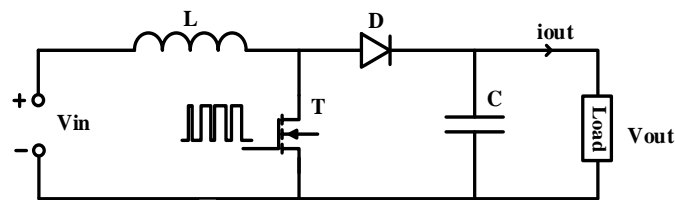


Figure 2. Electrical schematic of boost power converter

When designing a converter, it is essential to take into account the ripple current  $\Delta I_L$ , which is usually set at 10% of the inductor current  $i_L$  [22]. The converter's duty cycle  $\alpha$  is determined using the formula given in (1). The inductor value  $L$  is determined by the (2) where  $f$  represents the switching frequency,  $V_{in}$  and  $V_{out}$  represent respectively the input and output voltage of the converter, while the value of the capacitor  $C$  is calculated as shown in (3), where  $I_{out}$  is the current passing through the load. Table 1 summarizes the key parameters of the DC-DC boost converter. These parameters are calculated using the equations mentioned and are essential for correctly sizing the converter components.

$$\alpha = \frac{V_{out} - V_{in}}{V_{out}} \quad (1)$$

$$L = \frac{\alpha \times V_{in}}{f \times \Delta I_L} \quad (2)$$

$$C = \frac{\alpha \times I_{out}}{f \times \Delta V_{out}} \quad (3)$$

The analysis begins by extracting the state-space model for the boost converter, covering its operation in both ON and OFF modes, where R represents the resistive load. In (4) and (5) describe the system when the switch T is ON, while in (6) and (7) describe it when the switch T is OFF.

$$\frac{di_L}{dt} = \frac{1}{L} V_{in} \quad (4)$$

$$\frac{dV_{out}}{dt} = \frac{1}{C} * \left( -\frac{V_{out}}{R} \right) \quad (5)$$

$$\frac{di_L}{dt} = \frac{1}{L} * (V_{in} - V_{out}) \quad (6)$$

$$\frac{dV_{out}}{dt} = \frac{1}{C} * \left( i_L - \frac{V_{out}}{R} \right) \quad (7)$$

The state equations for a boost power converter in the ON state can be expressed as in (8), and when the switch T is OFF, the state equations can be written as in (9).

$$\begin{bmatrix} \frac{di_L}{dt} \\ \frac{dV_{out}}{dt} \end{bmatrix} = \begin{bmatrix} 0 & 0 \\ 0 & -\frac{1}{RC} \end{bmatrix} \begin{bmatrix} i_L \\ V_{out} \end{bmatrix} + \begin{bmatrix} \frac{1}{L} \\ 0 \end{bmatrix} V_{in} \quad (8)$$

$$\begin{bmatrix} \frac{di_L}{dt} \\ \frac{dV_{out}}{dt} \end{bmatrix} = \begin{bmatrix} 0 & -\frac{1}{L} \\ \frac{1}{C} & -\frac{1}{RC} \end{bmatrix} \begin{bmatrix} i_L \\ V_{out} \end{bmatrix} + \begin{bmatrix} \frac{1}{L} \\ 0 \end{bmatrix} V_{in} \quad (9)$$

Table 1. DC-DC boost converter main parameters

| Parameter        | Value        |
|------------------|--------------|
| V <sub>in</sub>  | [7 V-11.5 V] |
| V <sub>out</sub> | 12 V         |
| C                | 100 μF       |
| L                | 220 μH       |
| F                | 40 kHz       |
| R                | 100 Ω        |

To derive a converter model over a switching period, the state-space averaging technique is used. This method involves replacing the state space, which approximates circuit behavior over the whole period, with a state space that accurately captures circuit dynamics over a single switching period [23]. The resulting modified averaged model derived from this technique is represented by (10) and (11).

$$A = A_1 \times \alpha + A_2(1 - \alpha) \quad (10)$$

$$B = B_1 \times \alpha + B_2(1 - \alpha) \quad (11)$$

A<sub>1</sub>, A<sub>2</sub>, B<sub>1</sub>, and B<sub>2</sub> can be written as in (12) and (13).

$$A_1 = \begin{bmatrix} 0 & 0 \\ 0 & -\frac{1}{RC} \end{bmatrix} \quad A_2 = \begin{bmatrix} 0 & -\frac{1}{L} \\ \frac{1}{C} & -\frac{1}{RC} \end{bmatrix} \quad (12)$$

$$B_1 = \begin{bmatrix} \frac{1}{L} \\ 0 \end{bmatrix} \quad B_2 = \begin{bmatrix} \frac{1}{L} \\ 0 \end{bmatrix} \quad (13)$$

Using (10) and (11), we construct the average spatial state model of the converter over the entire period, as shown in (14).

$$\begin{bmatrix} \frac{di_L}{dt} \\ \frac{dV_{out}}{dt} \end{bmatrix} = \begin{bmatrix} 0 & -\frac{(1-\alpha)}{L} \\ \frac{(1-\alpha)}{C} & -\frac{1}{RC} \end{bmatrix} \begin{bmatrix} i_L \\ V_{out} \end{bmatrix} + \begin{bmatrix} \frac{1}{L} \\ 0 \end{bmatrix} V_{in} \quad (14)$$

The state vector is determined as in (15).

$$x = [i_L \ V_{out}]^T \quad (15)$$

The (15) can be written as in (16) and (17).

$$\dot{x} = Ax + BV_{in} \quad (16)$$

$$Y = Mx \quad (17)$$

Where Y is the output vector and  $A = \begin{bmatrix} 0 & -\frac{(1-\alpha)}{L} \\ \frac{1-\alpha}{C} & -\frac{1}{RC} \end{bmatrix}$   $B = \begin{bmatrix} \frac{1}{L} \\ 0 \end{bmatrix}$   $M = [0 \ 1]$ .

### 3. CONTROLLER DESIGN

#### 3.1. Sliding mode control

Sliding mode control (SMC) has been proven to be a robust non-linear control methodology, capable of handling the complex dynamics of variable structural systems. It offers significant advantages by assuring the stability and robustness of the system, even when its parameters fluctuate considerably. The SMC strategy consists of two distinct approaches [24]. In this paper, we are focusing on the concept of the approach mode [25] in which the control law is expressed in such a way as to control the state surface of the system in state space, with the aim of achieving the desired system behavior in a finite time. The system state variables are shown in (18).

$$X = \begin{bmatrix} X_1 \\ X_2 \\ X_3 \end{bmatrix} = \begin{bmatrix} V_{ref} - (\text{Beta} * V_{out}) \\ \frac{d}{dt}(V_{ref} - (\text{Beta} * V_{out})) \\ \int V_{ref} - (\text{Beta} * V_{out}) \ dt \end{bmatrix} \quad (18)$$

The voltage error, error derivative and error integral are represented by X1, X2 and X3, respectively. The specified voltage reference and voltage ratio divider to the converter output are indicated by Vref and Beta. Considering in (8), (9) and (15), in (18) can be reformulated as in (19).

$$X = \begin{bmatrix} X_1 \\ X_2 \\ X_3 \end{bmatrix} = \begin{bmatrix} V_{ref} - (\text{Beta} * V_{out}) \\ \frac{(\text{Beta} * V_{out})}{RC} + \frac{\text{Beta}}{LC} \int (V_{ref} - V_{in}) \alpha \ dt \\ \int V_{ref} - (\text{Beta} * V_{out}) \ dt \end{bmatrix} \quad (19)$$

The control system's state equation in vector space is expressed as in (20).

$$\begin{bmatrix} \dot{X}_1 \\ \dot{X}_2 \\ \dot{X}_3 \end{bmatrix} = \begin{bmatrix} 0 & 1 & 0 \\ 0 & -\frac{1}{RC} & 0 \\ 1 & 0 & 0 \end{bmatrix} \begin{bmatrix} X_1 \\ X_2 \\ X_3 \end{bmatrix} + \begin{bmatrix} 0 \\ \frac{(\text{Beta} * V_{out})}{RC} - \frac{(\text{Beta} * V_{in})}{LC} \\ 0 \end{bmatrix} \quad (20)$$

The switching function in the SMC law is expressed as in (21).

$$u = \begin{cases} 1, & \text{when } \gamma > 0 \\ 0, & \text{when } \gamma < 0 \end{cases} \quad (21)$$

The instantaneous trajectory of the state, represented by  $\gamma$ , is defined in (22).

$$\gamma = X_1\alpha_1 + X_2\alpha_2 + X_3\alpha_3 = J^T X \quad (22)$$

The (22) represents the sliding coefficients, where:  $J^T = [\alpha_1 \ \alpha_2 \ \alpha_3]$ .

To regulate the switch in a boost converter using pulse width modulation (PWM), a control mechanism is used where a  $V_c$  signal is compared with a sawtooth reference signal  $V_r$ . This comparison effectively determines the desired duty cycle of the PWM signal  $u_{eq}$ . The control signal is then processed by a PWM modulator to convert it into an appropriate duty cycle. This duty cycle directly determines the ON/OFF time ratio of switch in the system, as shown in Figure 3.

$$\dot{\Gamma} = J^T A X + J^T B \bar{u}_{eq} = 0 \quad (23)$$

$$\text{Were } \bar{u}_{eq} = -[J^T B]^{-1} J^T A X \quad (24)$$

$$\bar{u}_{eq} = \frac{\text{Beta} \cdot L \cdot \left( \frac{\alpha_1}{\alpha_2} - \frac{1}{RC} \right)}{\text{Beta} \cdot (V_{out} - V_{in})} I_c - \frac{\alpha_3 \cdot L \cdot C \cdot (V_{ref} - \text{Beta} \cdot V_{out})}{\alpha_2 \cdot \text{Beta} \cdot (V_{out} - V_{in})} \quad (25)$$

In this equation, condition  $0 < \bar{u}_{eq} < 1$  is defined by taking into account:

$$\bar{u}_{eq} = 1 - u_{eq} \quad (26)$$

In (24) can be expressed as (27), and  $u_{eq}$  can be presented by (28):

$$0 < u_{eq} = \frac{-I_c \cdot \text{Beta} \cdot L \cdot \left( \frac{\alpha_1}{\alpha_2} - \frac{1}{RC} \right) + \frac{\alpha_3 \cdot L \cdot C}{\alpha_2} \cdot (V_{ref} - \text{Beta} \cdot V_{out}) + \text{Beta} \cdot (V_{out} - V_{in})}{\text{Beta} \cdot (V_{out} - V_{in})} < 1 \quad (27)$$

$$0 < u_{eq} = \frac{V_c}{V_r} < 1 \quad (28)$$

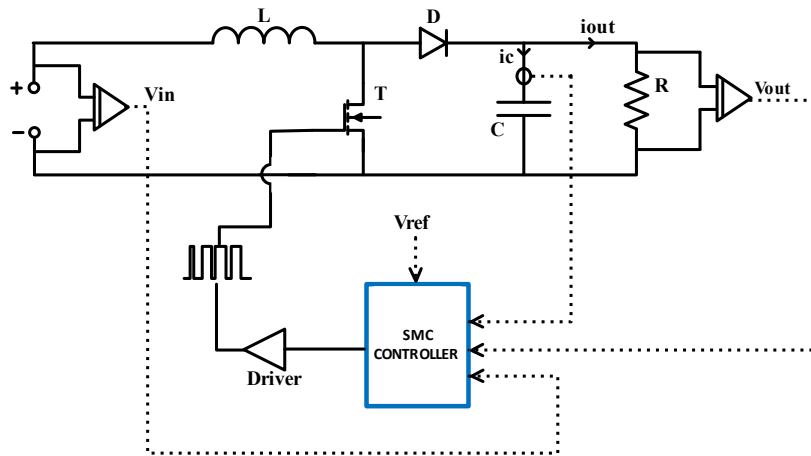


Figure 3. Schematic representation of boost converter using SMC

### 3.2. Fuzzy logic controller

Unlike conventional approaches, which are often limited by complex mathematical models, FLC is fundamentally built on linguistic control approaches derived from the knowledge of experts and translated into an automated decision-making process. This enables FLC to address a wide range of challenging control problems for which accurate modeling remains difficult to achieve. FLC is a revolutionary control algorithm that bridges the gap between human expertise and algorithmic control in complex systems [26]. The FLC controller has three principal components:

- Fuzzification: The transformation of input variables into linguistic variables involves the use of membership functions (MFs). Triangles and trapezoids are the types of membership functions most commonly used in the literature.
- Inferences: Generating fuzzified output based on defined rules, using the fuzzified input.
- Defuzzification: Converting fuzzy output into a precise control signal for the converter.

To adjust the DC/DC converter output voltage using a fuzzy logic controller (FLC), The FLC reads the output voltage value and calculates the error ( $e$ ) by comparing the current voltage with the target reference voltage. It also considers the rate of change of this error ( $\Delta e$ ). Based on this data, the FLC uses a table of fuzzy rules to define the duty cycle  $\alpha$  for the pulse width modulation (PWM) signal according to the schematic shown in Figure 4.

Table 2 displays the fuzzy rule table, which utilizes a set of "If...Then" rules to define the control strategy. These rules are expressed in natural language, making them easy to comprehend. Each input variable ( $e$  and  $\Delta e$ ) and the output variable ( $\alpha$ ) are characterized using linguistic terms: negative (N), zero (Z), and positive (P).

Table 2. Fuzzy logic rules

| $e$<br>$\Delta e$ | N | Z | P |
|-------------------|---|---|---|
| N                 | P | P | P |
| Z                 | P | Z | N |
| P                 | P | N | N |

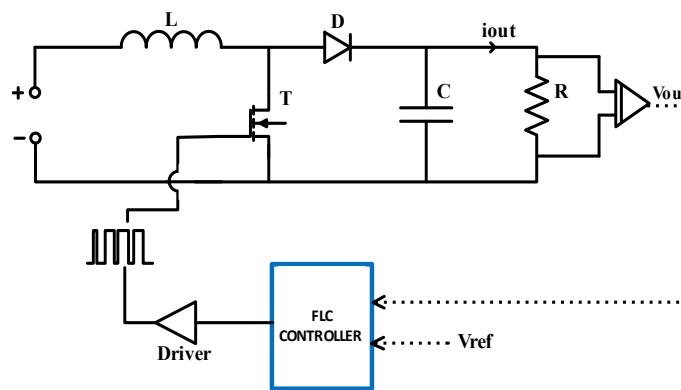


Figure 4. Schematic representation of boost converter using FLC

## 4. RESULTS ANALYSIS AND DISCUSSION

### 4.1. Simulation results

To validate the efficiency of the system using SMC and FLC, this section presents simulation results. Figures 5(a) and 5(b) show the output voltage response of the boost power converter under fuzzy logic control (FLC) and sliding mode control (SMC) respectively, with a variable input voltage profile and a load varying from  $100\ \Omega$  to  $80\ \Omega$  at  $0.08\text{ s}$ . Both controllers accurately track the  $12\text{ V}$  reference voltage, with peak overshoots of  $14.2\%$  for the FLC and  $0.39\%$  for the SMC. The root mean square error (RMSE) is  $0.14\text{ V}$  for the FLC and  $0.075\text{ V}$  for the SMC. Despite noticeable overshoots, both regulators show minor deviations from the reference, which are quickly attenuated by short settling times of  $6.4\text{ ms}$  for the FLC and  $4.2\text{ ms}$  for the SMC, highlighting their rapid response capabilities. The mean absolute percentage error (MAPE) also confirms the accuracy of the FLC ( $1.12\%$ ) and SMC ( $0.5\%$ ) in achieving the desired output voltage. Overall, the SMC controller outperforms the FLC controller in terms of overshoot, settling time, and accuracy.

### 4.2. Experimental results

The experimental test platform Figure 6 includes a programmable DC power supply to generate an output voltage profile. In addition, the platform includes a DC-DC boost power converter prototype designed to regulate output voltage, and a resistive load for testing. The LAUNCHXL-F28069M digital signal processor (DSP) (board serves as a platform for implementing either SMC or FLC. Signals are then generated by the board according to the controller selected to drive the DC-DC boost power converter. The various inputs and outputs demanded by the controller's algorithms, are captured using an LV25-P sensor for voltage detection and an LTS 25-NP sensor for current detection. Additionally, a Mastech MS8218 multimeter is used to visualize the output voltage and collect the data. This configuration enables real-time monitoring and data logging for comprehensive analysis and evaluation of boost power converter performance.

The converter parameters were selected similarly to the simulation study. Figures 7(a) and 7(b) illustrate a variable input voltage with a load change from  $80\ \Omega$  to  $100\ \Omega$  under FLC and SMC, respectively. The FLC controller in Figure 7(a) shows an overshoot of  $15.77\%$ , a settling time of  $44\text{ ms}$ , a MAPE of  $5.5\%$ , and an RMSE of  $0.66\text{ V}$ . The SMC controller in Figure 7(b) demonstrated a minimum overshoot of  $0.48\%$ , a

settling time of 9 ms, a MAPE of 2.08 %, and an RMSE of 0.25 V relative to the 12 V reference voltage. Overall, the SMC controller outperforms the FLC controller in terms of overshoot, settling time, and accuracy.

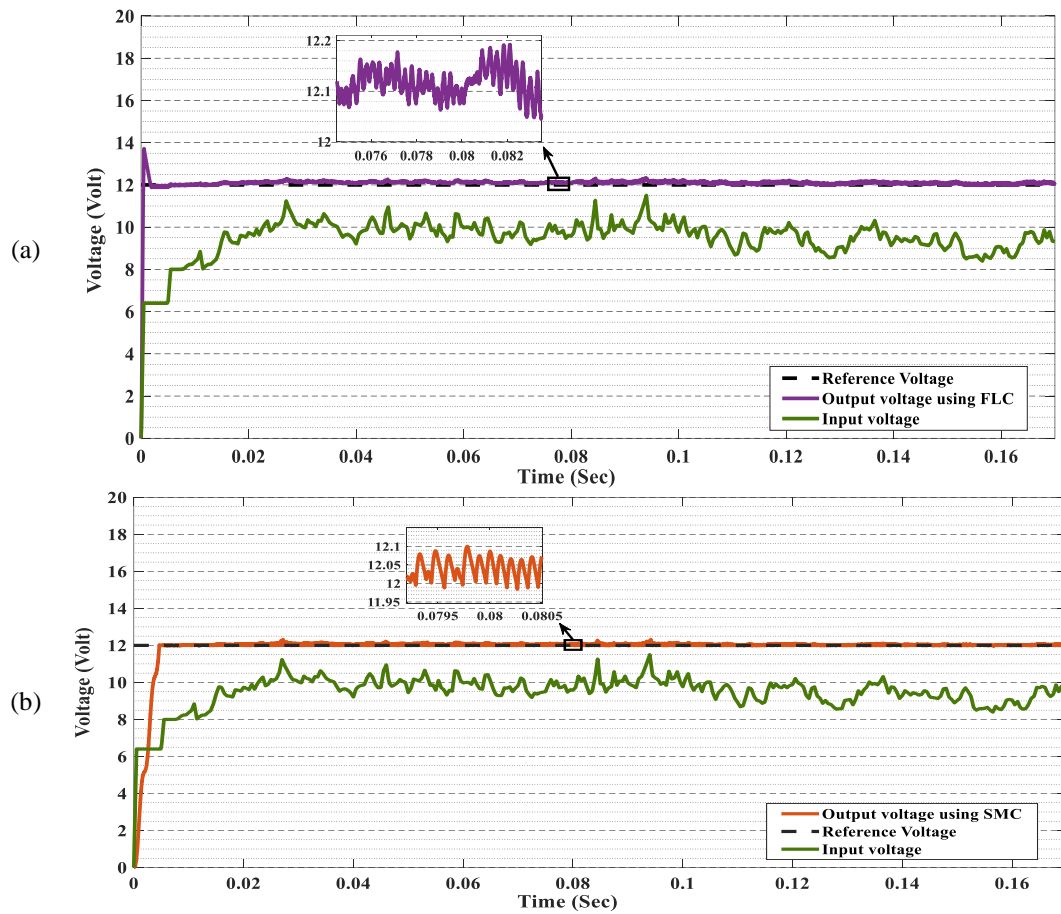


Figure 5. Simulation results of boost converter response with (a) FLC and (b) SMC

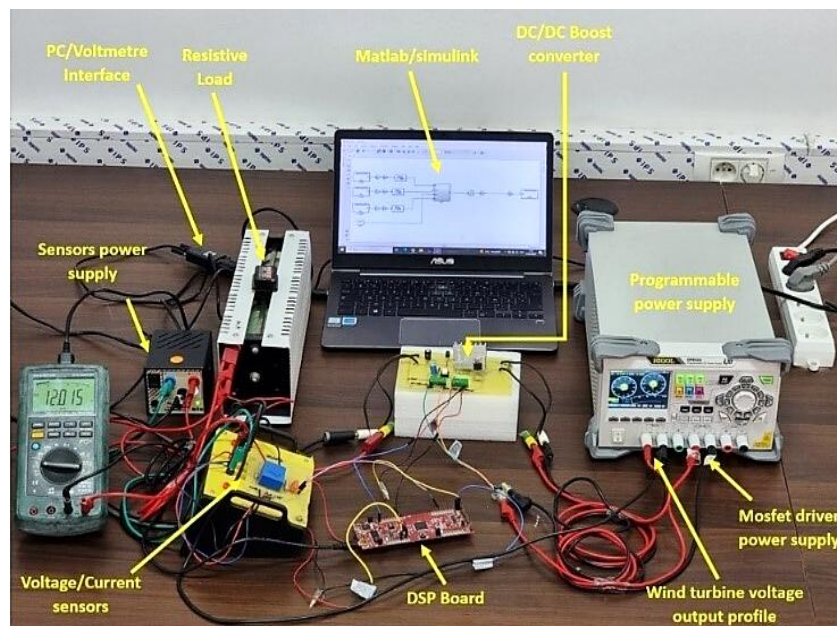


Figure 6. Experimental test platform setup



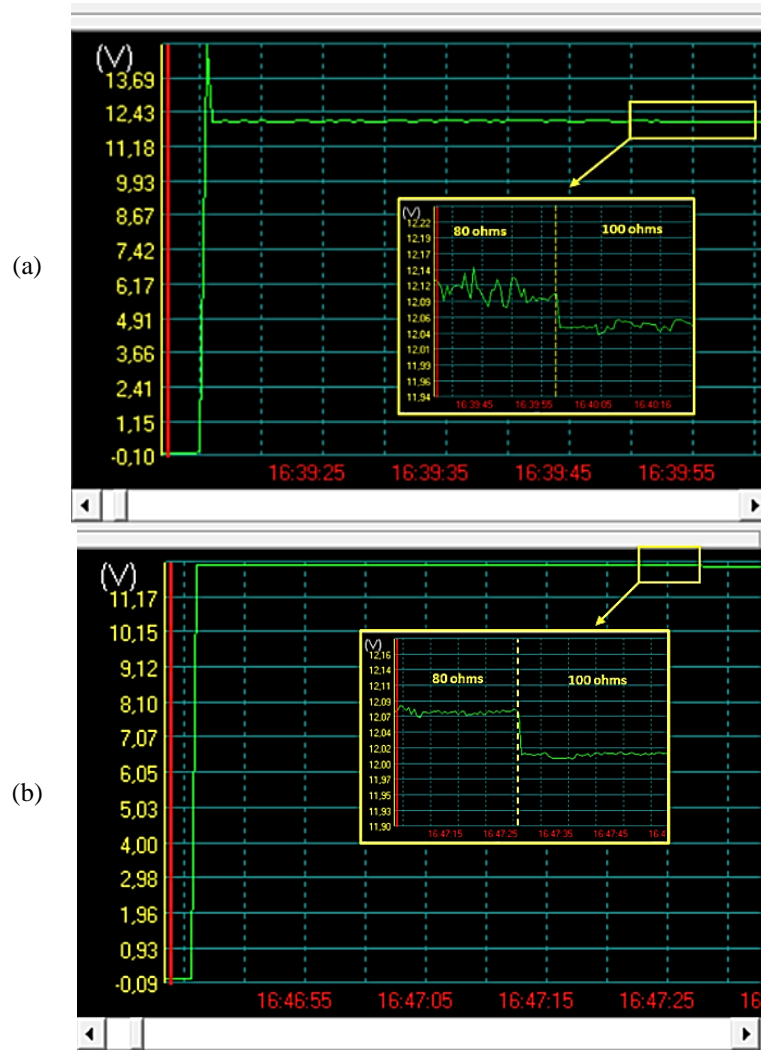


Figure 7. Experimental results of boost converter response with (a) FLC and (b) SMC

## 5. CONCLUSION

In this paper, we present an experimental validation of sliding mode control (SMC) and fuzzy logic control (FLC) applied to DC/DC boost power converters to adjust the output voltage produced of wind turbine systems. Our results demonstrate the advantages of sliding mode control over fuzzy logic control. During testing conducted on a physical prototype and a DSP board, SMC consistently shows superior performance in the context of peak overshoot, settling time, and mean absolute percentage error (MAPE). However, it's important to note that SMC can suffer from "chattering," which has an impact on component efficiency and durability. On the other hand, FLC exhibits longer settling times and higher peak overshoots. To maximize the effectiveness of SMCs in the real world, it is essential to address the phenomenon of chattering, which negatively affects the performance of the system. Similarly, optimizing FLC parameters or exploring alternative control strategies can improve its dynamic response and reduce stabilization time. These results demonstrate the importance of our study for the implementation of effective voltage regulation strategies in wind energy systems. By addressing the identified challenges and optimizing control strategies, we can further improve the reliability and performance of wind power systems.

## ACKNOWLEDGEMENTS

Authors may acknowledge any person, institution, or department that supported to any part of the study.






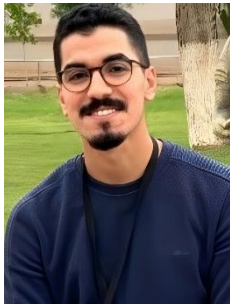
## REFERENCES




- [1] Z. Yu, W. Zheng, K. Zeng, R. Zhao, Y. Zhang, and M. Zeng, "Energy optimization management of microgrid using improved soft actor-critic algorithm," *International Journal of Renewable Energy Development*, vol. 13, no. 2, pp. 329-339, Feb. 2024, doi: 10.61435/ijred.2024.59988.
- [2] M. Lagouir, A. Badri, and Y. Sayouti, "Solving Multi-Objective Energy Management of a DC Microgrid using Multi-Objective Multiverse Optimization," *International Journal of Renewable Energy Development*, vol. 10, no. 4, pp. 911-922, Oct. 2021, doi: 10.14710/ijred.2021.38909.
- [3] M. S. Alam, F. S. Al-Ismael, A. Salem, and M. A. Abido, "High-level penetration of renewable energy sources into grid utility: Challenges and solutions," *IEEE Access*, vol. 8, pp. 190277-190299, Oct. 2020, doi: 10.1109/ACCESS.2020.3031481.
- [4] M. A. Hannan *et al.*, "Wind Energy Conversions, Controls, and Applications: A Review for Sustainable Technologies and Directions," *Sustainability*, vol. 15, p. 3986, Mar. 2023, doi: 10.3390/su15053986.
- [5] F. Blaabjerg, Y. Yang, K. A. Kim, and J. Rodriguez, "Power electronics technology for large-scale renewable energy generation," in *Proceedings of the IEEE*, vol. 111, no. 4, Apr. 2023, pp. 335-355, doi: 10.1109/JPROC.2023.3253165.
- [6] M. Mahmoud *et al.*, "A Novel Front-End Single-Stage Bridgeless Boost converter for Grid Integration of Multisource DC-Microgrid Applications," in *2022 IEEE Industry Applications Society Annual Meeting*, Houston, TX, USA, Oct. 2022, doi: 10.1109/IAS54023.2022.9939763.
- [7] A. Kheiter, S. Souag, A. Chaouch, A. Boukourt, B. Bekkouche, and M. Guezgouz, "Energy management strategy based on marine predators algorithm for grid-connected microgrid," *International Journal of Renewable Energy Development*, vol. 11, no. 3, pp. 751, 2022, doi: 10.14710/ijred.2022.42797.
- [8] S. K. H. Shah, A. Hellany, M. Nagrial, and J. Rizk, "Impact of wind speed on total harmonic distortion in a hybrid renewable energy system," in *2022 IEEE International Conference on Power Systems Technology (POWERCON)*, Chengdu, China, Sept. 2022, pp. 1-5, doi: 10.1109/POWERCON53406.2022.9929674.
- [9] M. Jan, E. Alam, K. Muttaqi, and D. Sutanto, "Battery Energy Storage to Mitigate Rapid Voltage/Power Fluctuations in Power Grids Due to Fast Variations of Solar/Wind Outputs," *IEEE Access*, vol. 9, pp. 305128-305138, Jan. 2021, doi: 10.1109/ACCESS.2021.3051283.
- [10] P. Albert and S. Y. Kim, "Transient Stability Analysis and Enhancement Techniques of Renewable-Rich Power Grids," *Energies*, vol. 16, no. 5, p. 2495, Mar. 2023, doi: 10.3390/en16052495.
- [11] K. Sharma and D. K. Palwalia, "Design of digital PID controller for voltage mode control of DC-DC converters," in *2017 International conference on Microelectronic Devices, Circuits and Systems (ICMDCS)*, 2017, pp. 1-6, doi: 10.1109/ICMDCS.2017.8211715.
- [12] A. Korompili and A. Monti, "Review of modern control technologies for voltage regulation in DC-DC converters of DC microgrids," *Energies*, vol. 16, no. 12, p. 4563, Jun. 2023, doi: 10.3390/en16124563.
- [13] S. A. Sanabria-Torres *et al.*, "Design of Proportional-Resonant Controllers for Voltage-Source Converters using State-Space Model," in *IECON 2021 – 47th Annual Conference of the IEEE Industrial Electronics Society*, Toronto, ON, Canada, Oct. 2021, pp. 1-6, doi: 10.1109/IECON48115.2021.9589113.
- [14] J. Loranca-Coutinho, J. C. Mayo-Maldonado, G. Escobar, T. M. Maupong, J. E. Valdez-Resendiz, and J. C. Rosas-Caro, "Data-driven passivity-based control design for modular DC microgrids," *IEEE Transactions on Industrial Electronics*, vol. 69, no. 3, pp. 2545-2556, 2021, doi: 10.1109/TIE.2021.3065615.
- [15] A. Kamran, M. Moradi, P. Zamani, and Q. Shafiee, "Data-driven predictive control of perturbed buck converters using a modified iterative feedback tuning algorithm," *IET Power Electron.*, vol. 17, no. 10, pp. 1314-1323, 2024, doi: 10.1049/pel2.12720.
- [16] S. Das, T. K. Gangula, R. Nizami, and R. Udumula, "Adaptive neural network control of DC-DC power converter," *Expert Systems with Applications*, 2023, doi: 10.1016/j.eswa.2023.120362.
- [17] M. BENYDIR *et al.*, "Implementation and analysis of a fuzzy logic and sliding mode controller on a boost DC/DC converter in a PV array," *International Journal of Renewable Energy Research (IJRER)*, vol. 13, no. 1, pp. 294-301, 2023, doi: 10.20508/ijrer.v13i1.13862.g8683.
- [18] T. Rahimi, M. R. Islam, H. Gholizadeh, S. Mahdizadeh, and E. Afjei, "Design and implementation of a high step-up dc-dc converter based on the conventional boost and buck-Boost power converters with high value of the efficiency suitable for renewable application," *Sustainability*, vol. 13, no. 19, p. 10699, Oct. 2021, doi: 10.3390/su131910699.
- [19] M. K. Shehata, H. E. M. Attia, N. F. Ibrahim, and B. Elnaghi, "Sliding-mode control for boost converters under voltage and load variations," *International Journal of Power Electronics and Drive Systems (IJPEDS)*, vol. 14, no. 3, pp. 1615-1623, Mar. 2023, doi: 10.11591/ijpeds.v14.i3.pp1615-1623.
- [20] A. AlZawaideh and I. Boiko, "Analysis of a sliding mode DC-DC Boost converter through LPRS of a nonlinear plant," *IEEE Transactions on Power Electronics*, vol. 35, no. 11, pp. 12321-12331, Nov. 2020, doi: 10.1109/TPEL.2020.2983596.
- [21] J. Narayanaswamy and S. Mandava, "Non-isolated multiport converter for renewable energy sources: A comprehensive review," *Energies*, vol. 16, no. 4, Feb. 2023, doi: 10.3390/en16041834.
- [22] J. L. Soon *et al.*, "Current Ripple Reduction Using AC Core Biasing in DC-DC Converters," *IEEE Transactions on Industrial Electronics*, vol. 68, no. 10, 2021, doi: 10.1109/TIE.2020.3021610.
- [23] P. Sharma, D. K. Dhaked, and A. K. Sharma, "Mathematical modeling and simulation of DC-DC converters using state-space approach," in *Proceedings of Second International Conference on Smart Energy and Communication. Algorithms for Intelligent Systems*, Springer Singapore, 2021, pp. 11-29, doi: 10.1007/978-981-15-6707-0\_2.
- [24] A. Jemmali, K. Elleuch, H. Abid, and A. Toumi, "Comparative study between PI and SMC controllers for DFIG using fuzzy wind power estimator," *International Journal of Power Electronics and Drive Systems (IJPEDS)*, vol. 14, no. 3, pp. 1748-1758, 2023, doi: 10.11591/ijpeds.v14.i3.pp1748-1758.
- [25] J. Hu, H. Zhang, H. Liu, and X. Yu, "A survey on sliding mode control for networked control systems," *International Journal of Systems Science*, vol. 52, no. 6, pp. 1129-1146, Jun. 2021, doi: 10.1080/00207721.2021.1890156.
- [26] A. H. Ahmed, B. K. Abd El Samie, and A. M. Ali, "Comparison between fuzzy logic and PI control for the speed of BLDC motor," *International Journal of Power Electronics and Drive Systems (IJPEDS)*, vol. 9, no. 3, pp. 1116-1123, 2018, doi: http://doi.org/10.11591/ijpeds.v9.i3.pp1116-1123.

## BIOGRAPHIES OF AUTHORS






**Belkasem Imodane**    is a Ph.D. student in electrical engineering at the University of Ibn Zohr, Agadir. He graduated as an embedded systems engineer in 2021 from the National School of Applied Sciences, Agadir, Morocco. Subsequently, he joined the research group at the Engineering Sciences and Energy Management Laboratory, University of Ibn Zohr, Agadir, Morocco. His research focuses on renewable energies for his doctoral thesis. He can be contacted at email: b.imodane@uiz.ac.ma.






**Mohamed Benydir**    is a Ph.D. candidate and substitute teacher specializing in Electrical Engineering at the High School of Technologies in Agadir (EST Agadir), originates from Agadir, Morocco. His research, integral to his national doctoral thesis, is primarily focused on renewable energy, engineering science, and energy management. He can be contacted at email: mohamed.benydir@edu.uiz.ac.ma.






**Brahim Bouachrine**    is professor Ph.D. at the Department of Electrical and Energy Engineering, High School of Technologies of Guelmim (ESTG), Ibn Zohr University, Morocco. His research interests are in renewable energy: photovoltaic and wind energy systems, photovoltaic emulators, hybrid MPPT control, system modeling, and power electronics. He can be contacted at email: b.bouachrine@uiz.ac.ma.



**Mohamed Ajaamoum**    is a professor Ph.D. at the Department of Electrical Engineering, High School of Technology of Agadir, Ibn Zohr University, Agadir, Morocco. His research interests include photovoltaic systems, fuzzy control, neural networks, renewable energy technologies, system modeling, and power electronics. He can be contacted at email: m.ajaamoum@uiz.ac.ma.



**Kaoutar Dahmane**    is a Ph.D. student in Engineering Sciences at the Ibn Zohr University (UIZ) of Agadir. She is originally from Ouarzazate, Morocco. As a research student, she addresses key questions in relation to power system and renewable energy. The main aim of her doctoral thesis is to perform power quantity and quality controls in grid-connected renewable energy systems. She can be contacted at email: kaoutar.dahmane@edu.uiz.ac.ma.